

BiNSGPS: Geometry Problem Solving via Bidirectional Neuro-Symbolic Interaction

Qi Wang^{1,2*}, Peijie Wang^{1,2*}, Fei Yin^{1,2}, Cheng-Lin Liu^{1,2†}

¹MAIS, Institute of Automation of Chinese Academy of Sciences

²School of Artificial Intelligence, University of Chinese Academy of Sciences

wangqi226@mails.ucas.ac.cn wangpeijie2023@ia.ac.cn

{fyin, liucl}@nlpr.ia.ac.cn

Abstract

Geometry problem solving poses distinct challenges in artificial intelligence. Existing approaches typically fall into two paradigms: symbolic methods, which exhibit limited adaptability, and neural methods, which are prone to hallucinations. Recent neuro-symbolic hybrids predominantly rely on a unidirectional pipeline where neural outputs are fed into solvers without feedback, making system brittle to early-stage errors. To break this unidirectional bottleneck, we propose BiNSGPS, a framework that establishes Bidirectional Neuro-Symbolic Interaction (BiNS) between a MLLM Adviser and a Symbolic Solver. MLLM Adviser actively incorporates feedback from the symbolic solver to dynamically rectify inconsistent formal representations or propose auxiliary hypotheses, resolving symbolic conflicts and facilitating complex deductions. Experiments show that BiNSGPS achieves state-of-the-art performance, reaching 90.5% completion accuracy on Geometry3K and 90.1% on PGPS9K, while maintaining 96% step-wise logical coherence to balance capability with mathematical rigor.

1 Introduction

Geometry Problem Solving (GPS) stands as a quintessential challenge in artificial intelligence, serving as a rigorous task for evaluating high-level cognitive synthesis (Trinh et al., 2024; Wang et al., 2025b; Zhang et al., 2024a). Mainstream GPS approaches traditionally diverge into two paradigms: **symbolic methods** and **neural methods** (Zhang et al., 2023; Li et al., 2024b; Zhang et al., 2024c). Symbolic methods offer high precision and logical rigor (Lu et al., 2021; Zhang et al., 2024d, 2025), yet they are hampered by a significant formalization bottleneck. Translating raw problems into structured representations heavily depends on human annotations, and since symbolic

methods are highly sensitive to initial parsing errors, incorrect automated formalization will lead to system collapse (Wu et al., 2022; Gan and Yu, 2018; Li et al., 2024a). Furthermore, the reasoning scope of symbolic systems is inherently restricted by predefined theorem rule sets, limiting their adaptability to diverse geometric configurations (Fu et al., 2025a; Ping et al., 2025). Conversely, neural methods—ranging from specialized networks to Multimodal Large Language Models (MLLMs)—demonstrate superior flexibility by directly ingesting multimodal inputs (Li et al., 2024b; Gao et al., 2023; Shi et al., 2024; Chen et al., 2025; Gao et al., 2024; Zhu et al., 2025; Wang et al., 2025a). However, these models are notoriously susceptible to **hallucinations**; they often generate superficially plausible yet logically flawed deductions, which severely undermines their mathematical credibility.

Recently, neuro-symbolic methods have emerged as a promising direction to synergize the multimodal comprehension of neural models with the rigorous deduction of symbolic engines (Yang et al., 2025; yi chen et al., 2026). However, current frameworks predominantly rely on a unidirectional pipeline, where neural models serve as front-end parsers to translate multimodal inputs into formal representations for a back-end symbolic solver (Ping et al., 2025). This architecture creates a critical vulnerability: the information flow is strictly forward-moving, leaving the symbolic engine as a passive recipient of potentially flawed inputs. In complex geometric scenarios, neural formalization is notoriously prone to perceptual errors, while symbolic engines are often constrained by the inherent incompleteness of predefined theorem sets. Without a bidirectional feedback mechanism to "talk back" from the reasoning stage, the system lacks the agency to either rectify parsing hallucinations or leverage neural intuition to augment reasoning when the symbolic solver

* Equal contribution.

† Corresponding author.

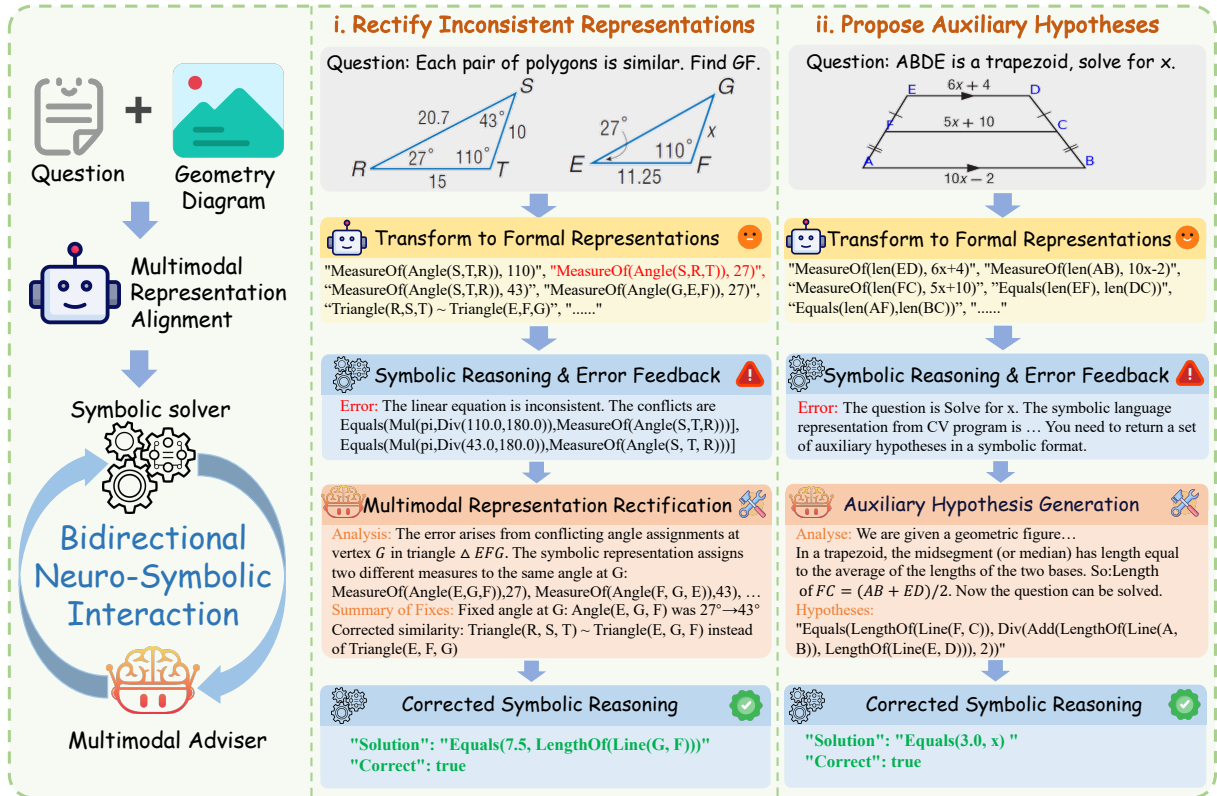


Figure 1: **Overview of our BiNSGPS.** BiNSGPS processes multimodal inputs (text and diagram) through an iterative reasoning loop. Upon detecting inconsistencies (Case i: conflicting angle measures) or missing constraints (Case ii: trapezoid properties), the MLLM Adviser triggers representation rectification or auxiliary hypothesis generation. The two examples on the right illustrate how the closed-loop feedback transforms initial attempts (marked with **red warnings**) into verified solutions (**green checks**).

reaches a deadlock. Consequently, even a minor initial representation error or a missing theorem can lead to the failure of the entire reasoning chain.

To address these bottlenecks, we propose **BiNSGPS**, a novel framework that reformulates the neuro-symbolic paradigm as an MLLM-based agentic tool-calling architecture. Central to our approach is the **Bidirectional Neuro-Symbolic Interaction (BiNS)**, which breaks the traditional unidirectional constraint by establishing an active feedback loop between the MLLM Adviser and the Symbolic Solver, thereby enabling a bidirectional flow of information. Within this closed-loop system, the Symbolic Solver performs rigorous deduction via hypergraph expansion, identifying logical inconsistencies or deductive deadlocks. Specifically, BiNS enables the Symbolic Solver to generate diagnostic feedback that triggers the MLLM Adviser to either rectify inconsistent formal representations or propose auxiliary hypotheses derived from the MLLM’s internal knowledge, effectively circumventing the limitations of predefined theorem rule sets. As illustrated in Fig. 1, the MLLM Adviser can dynamically correct perceptual errors

identified by the Symbolic Solver or introduce external geometric intuition to break reasoning deadlocks. Comprehensive experiments demonstrate that BiNSGPS achieves state-of-the-art (SOTA) accuracies while effectively balancing mathematical rigor with reasoning flexibility.

Our contributions are summarized as follows:

1. Interactive Correction and Augmentation: We introduce **BiNS** mechanism into neural-symbolic methods, where the Symbolic Solver provides diagnostic feedback to MLLM Adviser. This interaction enables rectification of formalization errors and heuristic augmentation of reasoning.

2. Bidirectional Neuro-Symbolic Framework: We propose **BiNSGPS**, reformulating the traditional unidirectional neuro-symbolic pipeline into an agentic, tool-calling architecture. By establishing a feedback loop between the MLLM Adviser and the Symbolic Solver, we break the rigid information bottleneck inherent in conventional GPS.

3. SOTA Performance: Extensive evaluations on Geometry3K and PGPS9K demonstrate that BiNSGPS achieves new SOTA performance, reaching 90.5% and 90.1% solving accuracy. BiNSGPS

also ensures exceptional logical consistency in step-wise deductions, establishing a superior balance between reasoning flexibility and mathematical rigor.

2 Related Work

2.1 Geometry Problem Solving

Geometry Problem Solving (GPS) is a hallmark of mathematical intelligence. Existing literature can be broadly categorized into three paradigms: 1. Neural-based methods treat GPS as a visual question answering task. Early works utilized specialized architectures like PGPSNet (Zhang et al., 2022) and LANS (Li et al., 2024b), while recent efforts leverage the reasoning power of MLLMs such as G-LLaVA (Gao et al., 2023) and Vision-R1 (Huang et al., 2026). While these models excel at flexible intuition, they are prone to hallucinations and lack the rigor required for mathematical proofs. 2. Symbolic-based methods (e.g., InterGPS (Lu et al., 2021), E-GPS (Wu et al., 2024)) translate raw inputs into structured formal languages and execute deduction. Although logically rigorous, these systems suffer from a formalization bottleneck: they are highly sensitive to initial parsing errors and lack the adaptability to handle configurations outside their hard-coded theorems. 3. Neuro-symbolic methods attempt to bridge this gap. Recent breakthroughs like AlphaGeometry (Trinh et al., 2024) and AlphaGeometry2 (Chervonyi et al., 2025) combine language models with symbolic engines to solve Olympiad problems. Other approaches like AutoGPS (Ping et al., 2025) and GeoDRL (Peng et al., 2023) use MLLM components to guide theorem selection or generate aligned representations. Geoparsing (Wang et al., 2026) further advances the perception stage by introducing a unified formal language for both plane and solid geometry diagram parsing, enabling MLLMs to convert geometric diagrams into structured symbolic descriptions that can serve as cognitive scaffolds for downstream reasoning. However, these systems predominantly rely on a unidirectional pipeline where the Symbolic Solver is a passive recipient of neural network outputs. This one-way flow means any parsing error is irrecoverable and the solver cannot "talk back" to the neural component for help. In contrast, our BiNSGPS framework introduces a bidirectional interaction. By establishing a feedback mechanism, the Symbolic Solver can prompt the MLLM to rectify inconsistent representations and hypothesize auxiliary constructions, breaking the "one-way" bottleneck of previous neuro-symbolic methods.

2.2 MLLMs for Geometry Reasoning

Multimodal Large Language Models (MLLMs) have become a focal point for mathematical reasoning, with specialized benchmarks such as Math-Vista (Lu et al., 2024), MATH-Vision (Wang et al., 2024), GeoEval (Zhang et al., 2024b), MV-MATH (Wang et al., 2025a), SolidGeo (Wang et al., 2025b) and GeoLaux (Fu et al., 2025b), highlighting their potential. Research in this area primarily follows two parallel trajectories. One direction focuses on Supervised Fine-Tuning and Reinforcement Learning (Xu et al., 2024a,b; Shao et al., 2024, 2025) to adapt models to the geometry domain, resulting in models like G-LLaVA (Gao et al., 2023) and GeoGPT4V (Cai et al., 2024). While these models exhibit improved intuition, they remain susceptible to both perceptual errors in diagram parsing and logical hallucinations during the deduction process. Another research trajectory treats MLLMs as agents that interact with external tools to solve complex tasks (Gou et al., 2024; Surís et al., 2023; Pan et al., 2023). Frameworks such as Visual SKETCHPAD (Hu et al., 2024) and CODEPLOT-COT (Duan et al., 2025) exemplify this approach, utilizing auxiliary drawing modules or code-execution environments to assist the MLLM in visual analysis and calculation.

In this work, we follow the agent-based paradigm by adopting a tool-calling architecture. Within the BiNSGPS framework, MLLM acts as a central coordinator that interfaces with specialized neural network and symbolic solvers. This approach allows the MLLM to leverage the high-fidelity outputs of domain-specific tools while focusing on strategy and error correction.

3 Methodology

3.1 Overview

The BiNSGPS framework is illustrated in Fig. 2. Our BiNSGPS framework is a closed-loop neuro-symbolic system comprising three primary components: Multimodal Representations Alignment, Symbolic Solver, and MLLM Adviser. The system follows an iterative execution flow to bridge the gap between neural intuition and symbolic rigor. Given a geometry problem $(\mathcal{D}, \mathcal{T})$, the diagram \mathcal{D} and text \mathcal{T} are first processed by the Multimodal Representations Alignment module to generate a formal specification in the form of an initial representations set $\mathcal{L} = (l_1, l_2, \dots, l_n)$, which serves as the foundational geometric facts for the problem.

The Symbolic Solver then ingests \mathcal{L} to perform

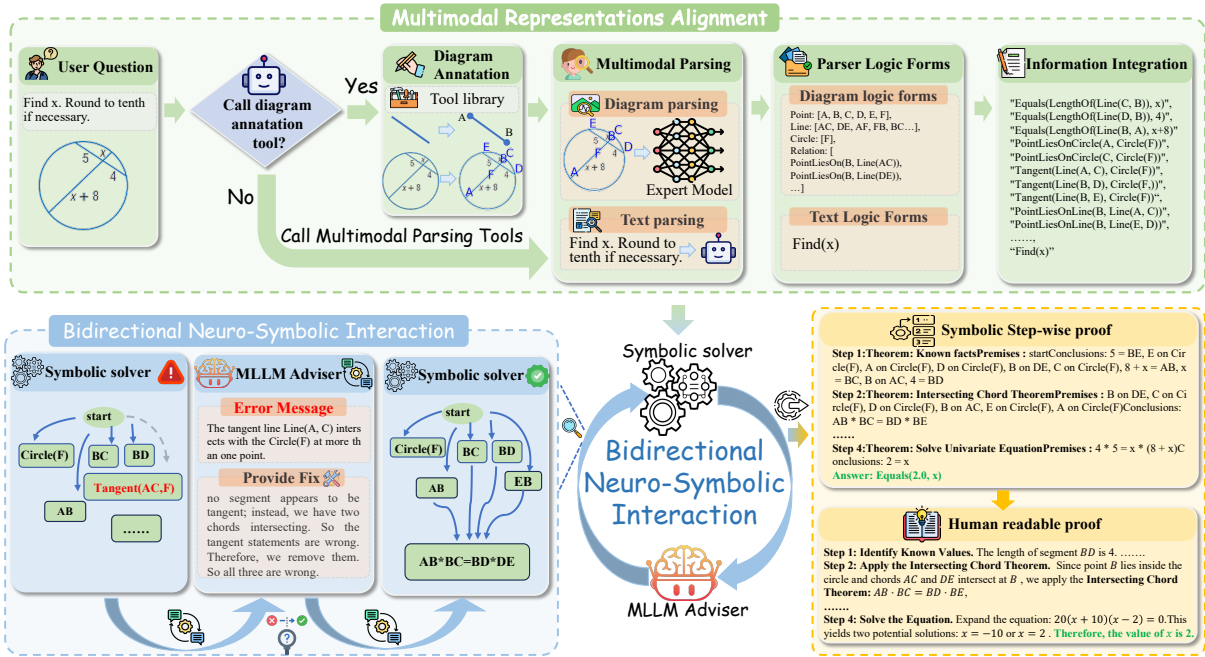


Figure 2: Framework of BiNSGPS pipeline. **Top**: Multimodal Representations Alignment. Geometry diagram-text pairs first get annotation. Then the pair are processed through a dual-parser architecture where a specialist neural network extracts structural diagram primitives while an MLLM parses textual constraints. These are integrated into initial logic forms \mathcal{L} , which are aligned and completed to form a comprehensive symbolic representation. **Bottom**: Bidirectional Neuro-Symbolic Interaction & Proof Generation. The Symbolic Solver constructs hypergraph for deductive reasoning. Upon encountering inconsistencies or deadlocks, the MLLM Adviser analyzes error diagnostics to rectify erroneous formalizations or propose auxiliary hypotheses \mathcal{H} . Once a solution is reached, the Solver identifies the minimal reasoning subgraph, which the MLLM subsequently translates into a human-readable proof.

deduction. Equipped with a predefined theorem rule set R , the solver formulates the reasoning process as a hypergraph expansion task. If the solving fails (including deductive deadlock or logical contradictions), it triggers the Bidirectional Feedback mechanism. The Symbolic Solver summarizes the current state and communicates it to the MLLM Adviser. In the case of conflict, the Adviser identifies and rectifies the inconsistent elements within \mathcal{L} based on the solver’s error trace to resolve inconsistency. If the solver reaches a deadlock, the Adviser analyzes the state to propose a hypothesis set \mathcal{H} . These auxiliary representations are provided as a supplement to \mathcal{L} , enabling the Symbolic Solver to bypass the "limited theorem" bottleneck.

This bidirectional loop continues until a verifiable solution is found or the maximum iteration limit is reached. If problem solved, the Symbolic Solver extract a minimal solution path, and then the MLLM polishes the solution into a human-readable format. If reach the iteration limit, the system employs a fallback mode, where the MLLM generates a direct numerical answer based on the existing representations. The details of each component are elaborated in the following sections.

3.2 Multimodal Representations Alignment

The Multimodal Representations Alignment module transforms diagrams \mathcal{D} and text \mathcal{T} into a unified set of formal symbolic representations. This process is carried out by the MLLM through tool invocation across three stages: Standardized Annotation, Dual-Source Extraction, and Unified Information Integration.

In the standardized annotation stage, the diagram is standardized for precise geometric extraction. The MLLM first evaluates the diagram to identify critical unlabeled features. If necessary, it invokes a specialized small-scale neural model to label points with unique letter identifiers. This results in an annotated diagram \mathcal{D}' , which ensures that all subsequent symbolic references are consistent across the vision and text modules.

In the dual-source extraction stage, the system extracts geometric facts from both visual and textual sources. The MLLM invokes PGDPNet to parse \mathcal{D}' . By leveraging PGDPNet’s superior accuracy ($> 99\%$) in element and position relation recognition, the system compensates for the inherent perceptual fragility of general-purpose MLLMs. This sub-module extracts basic elements \mathcal{B} (points,

lines, circles), positional relations \mathcal{P} (e.g., point on line) and other geometry representations \mathcal{F} . For the textual extraction, the MLLM acts as a text parser via few-shot prompting to extract textual assertions \mathcal{T}' . To resolve references like "quadrilateral in the figure," the MLLM is provided with \mathcal{D}' to align textual descriptions with visual grounding. The combined output is structured into a standardized JSON, encompassing \mathcal{B} , \mathcal{P} , additional formal assertions \mathcal{F} , and processed text \mathcal{T}' .

In information integration and transformation stage, The MLLM performs a holistic analysis of the extracted components to synthesize the final representation set \mathcal{L} . Crucially, the MLLM is instructed to prioritize the high-fidelity visual facts (\mathcal{B} and \mathcal{P}) from the diagram parser to calibrate and rectify potential errors in the textual extraction \mathcal{T}' .

3.3 Symbolic Solver

Upon receiving the initial representation set \mathcal{L} from the alignment module, the Symbolic Solver initiates a structured deduction process. Symbolic Solver formulate GPS as a Hypergraph Construction task, where geometric facts are represented as nodes and theorems as hyperedges. The solving procedure is executed in two primary stages: Geometric Completion and Iterative Graph Expansion.

Before formal deduction, the solver performs a completion step to ensure the initial representation set is logically complete and standardized. This stage automates the derivation of implicit properties from given definitions to ensure that subsequent reasoning is not stalled by missing foundational facts. After completion, the solver proceeds to the graph construction stage.

In graph expansion stage, the initial representations \mathcal{L} are treated as root nodes. The reasoning process is governed by a comprehensive theorem library \mathcal{R} , which includes geometric rules and algebraic rules. For each derivation, the solver identifies a minimal feasible set of nodes $m \subset \mathcal{L}'$ that satisfies the antecedents of a theorem rule $r \in \mathcal{R}$. The conclusion \mathcal{C} is then integrated into the graph as a new node. To ensure logical traceability and prevent circular reasoning, each node \mathcal{C} maintains a directed pointer to its parent nodes m and the specific rule r applied.

Throughout the process, the solver maintains strict logical integrity. If the solver detects a conflict, it immediately halts the derivation to prevent the propagation of errors. This terminal failure state, along with cases of deductive deadlock where

no new nodes can be generated, triggers the transition to the Bidirectional Feedback phase to resolve the underlying representational issues.

3.4 Bidirectional Feedback & MLLM Adviser

The MLLM Adviser serves as the sophisticated cognitive coordinator of the BiNSGPS framework, transforming the traditionally passive role of MLLMs into an active, agentic component capable of responding to the rigorous demands of Symbolic Solver. By establishing a closed-loop interaction, the Adviser addresses the "unidirectional bottleneck" that renders conventional neuro-symbolic systems brittle to early-stage errors. This bidirectional communication allows the system to operate in two distinct strategic modes—Rectify Inconsistent Representations and Propose Auxiliary Hypotheses—each triggered by specific failure states identified during the Symbolic Solver’s solving process.

In rectify inconsistent representations mode, which addresses logical contradictions, MLLM Adviser functions as a diagnostic and corrective agent. When the Symbolic Solver identifies an inconsistency, the conflict predication, including the annotated diagram \mathcal{D}' , text \mathcal{T} , and the conflicting initial representation set \mathcal{L} , is passed to the MLLM Adviser. To provide a stable foundation for this correction, we leverage the high-fidelity output of the PGDPNet diagram parser, designating the basic geometric elements \mathcal{B} and their positional relations \mathcal{P} as anchored ground truths. MLLM uses them as an objective reference to calibrate and refine more ambiguous assertions. In this rectification phase, the Adviser is strategically constrained to the modification or deletion of existing representations in \mathcal{L} , ensuring that the resubmitted representation set is a more accurate reflection of the raw geometric input rather than a hallucinated expansion.

When the Symbolic Solver reaches deductive deadlock—a state where no further theorems from the library \mathcal{R} can be applied—the Adviser transitions into Propose Auxiliary Hypotheses. This mechanism addresses the inherent limitation of symbolic systems, which are strictly bound by the scope of their predefined rule sets. Conversely, the MLLM can draw upon an expansive repository of geometric and algebraic knowledge acquired during its extensive pretraining, allowing it to propose novel conclusions \mathcal{H} that serve as vital catalysts for the solver. In this mode, the system prioritizes problem-solving by prompting the MLLM to gen-

erate supplementary representations that bridge the gap between known facts and the target answer. To mitigate the risk of creative hallucinations, we enforce a Rationale-Conclusion sequence; the MLLM must articulate an analytical reasoning chain before presenting any new formal representation. If the Symbolic Solver subsequently detects a conflict within this new hypothesis set \mathcal{H} , the error is immediately fed back to the Adviser for iterative refinement, creating a self-correcting cycle that persists until reaching a consistent and solvable state.

By synergizing the logical rigor of hypergraph deduction with the adaptive intuition of MLLM, the Adviser creates a new paradigm of deep integration, enabling the system to transcend the limitations of neural-based and symbolic-based approaches.

3.5 Proof Generation

The final stage of the BiNSGPS ensures that the derived results are both mathematically verifiable and human-readable. This process is bifurcated based on the outcome of the iterative reasoning loop: either generating a refined proof from the symbolic trace or executing a fallback procedure.

Upon the successful derivation of the target value, the Symbolic Solver performs a recursive back-trace to find the minimal solution graph, details can be found in the Appendix.C. The initial format is not suitable for human. To bridge this gap, the MLLM acts as a translator, converting the symbolic nodes and theorem applications into a more readable proof S' . This ensures that the final output maintains high logical alignment with the symbolic engine while friendly to users.

When the bidirectional interaction reaches the maximum iteration threshold, the system enters the fallback mode. In this mode, the MLLM is provided with the textual description \mathcal{T} , the annotated diagram \mathcal{D}' , and the high-accuracy basic geometric elements \mathcal{B} and positional relations \mathcal{P} . The MLLM is then prompted to provide the final output in a structured Analyze-Answer-Proof format. This ensures that when the solver cannot find a solution, the Adviser can provide an informed estimate supported by the structured visual grounding.

4 Experiments

To evaluate the effectiveness of BiNSGPS, we utilize two primary benchmarks in the geometry reasoning field: Geometry3K (Lu et al., 2021) and PGPS9K (Zhang et al., 2023), which provide 3,001 and 9,022 geometry problem-image pairs, respectively. Each problem is formatted with four candi-

date choices. We assess our framework under two distinct settings: Choice mode, where the model selects from the provided options, and Competition mode, where the system must derive the exact numerical answer independently. We also introduce a human-evaluation focused on Step-wise Logical Coherence. This metric is used to quantify the impact of MLLM hallucinations on the reasoning process, proving that the generated proofs are not merely superficially plausible but are mathematically sound to the symbolic derivations.

4.1 Comparison with State-of-the-art Solvers

As summarized in Table 1, BiNSGPS achieves a decisive performance advantage over state-of-the-art neural, symbolic, and multimodal large language models (MLLMs). In Choice mode, it outperforms the next best approach by 10.7% on Geometry3K and 10.9% on PGPS9K, reaching an accuracy of 95.2%. This is largely because BiNSGPS utilizes candidate choices as a verification signal: if the symbolic output mismatches the options, the MLLM Adviser is triggered to rectify proof trace errors, avoiding the random selection typical of traditional solvers. Notably, in the challenging Completion mode on Geometry3K, BiNSGPS achieves 90.5% accuracy, significantly surpassing frontier models like GPT-5.2 (77.9%).

Despite their rapid evolution, pure MLLMs like GPT-5.2 fail to breach the 80% accuracy threshold. This stems from a fundamental limitation in geometric grounding rather than visual resolution. Standard MLLM vision encoders employ a “semantic-first” tokenization that sacrifices spatial granularity for global context, leading to “perceptual drift” and missed mathematical precision. In contrast, BiNSGPS bridges this gap by offloading structural recognition to PGDPNet, which extracts rigorous geometric primitives. By anchoring the MLLM Adviser in this high-fidelity symbolic foundation, BiNSGPS eliminates pure-neural hallucinations, allowing the MLLM to focus on high-level reasoning while the Symbolic Solver guarantees mathematically valid deductions.

4.1.1 Step-wise Logical Coherence

While MLLMs can often arrive at a correct final answer through heuristic “shortcuts,” their internal reasoning is frequently marred by logical hallucinations. To assess the impact of the MLLM on problem solving within BiNSGPS, we conduct a human evaluation of step-wise correctness on 100 questions of Geometry3K. The accuracy of com-

Table 1: Performance comparison among state-of-the-art geometry problem solvers.

Method	Geometry3K		PGPS9K	
	Choice	Completion	Choice	Completion
MLLMs				
InternVL2.5-78B (Zhu et al., 2025)	60.9	36.1	51.3	28.1
Vision-R1-7B (Huang et al., 2026)	57.1	43.8	49.6	36.8
GPT-4o (OpenAI, 2024)	57.1	46.3	46.0	37.2
Qwen3-VL-7B (Bai et al., 2025)	50.1	44.8	44.9	43.0
Qwen2.5-VL-32B (Qwen et al., 2025)	58.6	46.3	56.1	43.5
InternVL3-78B (Zhu et al., 2025)	74.5	57.4	61.1	48.9
Qwen3-VL-Plus (Bai et al., 2025)	67.4	59.8	72.2	58.4
GPT-5.2	84.5	77.9	78.1	72.5
Neural Solvers				
NGS (Chen et al., 2021)	58.8	35.3	46.1	34.1
Geoformer (Chen et al., 2022)	59.3	36.8	47.3	35.6
PGPSNet (Zhang et al., 2023)	77.9	65.2	69.4	62.7
LANS (Li et al., 2024b)	82.3	72.1	74.0	66.7
Symbolic Solvers				
InterGPS (Lu et al., 2021)	63.5	50.6	66.2	57.4
E-GPS (Wu et al., 2024)	67.9	-	-	-
GeoDRL (Peng et al., 2023)	68.4	-	-	-
Neural-Symbolic Solvers				
GNS (LLaVA-1.5-13B) (Ning et al., 2025)	53.8	-	-	-
Pi-GPS (Zhao et al., 2025)	77.8	70.6	69.8	61.4
AutoGPS (Qwen3-VL-Plus) (Ping et al., 2025)	81.1	74.8	81.8	75.7
AutoGPS (GPT-4o) (Ping et al., 2025)	81.6	75.4	81.5	75.3
BiNSGPS (Qwen3-VL-Plus)	95.2	90.5	92.7	90.1
BiNSGPS (Qwen3-VL-32B)	90.3	87.0	89.2	87.6

mon MLLMs and BiNSGPS is reported in Table 2.

Table 2: Step-wise Logical Coherence and Multimodal Representations Alignment

MLLM model	Step Accuracy	Alignment
Qwen2.5-VL-32B	66.0%	-
Qwen3-VL-32B	-	56.0%
GPT-4o	70.0%	60.0%
Qwen3-VL-Plus	78.0%	58.0%
Ours (BiNSGPS)	96.0%	80.0%

The evaluation reveals a significant disparity in reasoning quality. Even advanced models like Qwen3-VL-Plus exhibit a "hallucination gap," with nearly 22% of their successful solutions containing at least one logically invalid step. In contrast, BiNSGPS achieves a coherence rate of 96.0%. This superior rigor is a direct result of our multi-layered validation architecture: the high-fidelity visual grounding of PGDPNet, the rigorous constraint-checking of the Symbolic Solver.

4.1.2 MathVista benchmark

To further evaluate BiNSGPS, we evaluated performance on the MathVista GPS part (Lu et al., 2024) against models from the official leaderboard, and the result is shown in Figure 3(a).

As shown in the figure, our BiNSGPS get 92.9, outperforming industry leaders like Kimi-k1.6 and Step R1-V. It is surpassed only by DreamPRM (95.7), which relies on a Process Reward Model. Notably, BiNSGPS is a tuning-free architecture, demonstrating that state-of-the-art reasoning can be achieved through bidirectional interaction without the overhead of specialized training or the risk of degrading the MLLM’s general capabilities.

4.2 Ablation Study

To analyze the effectiveness of each component within the BiNSGPS framework, we conduct a series of ablation studies. These studies focus on Multimodal Representation Alignment and the MLLM Adviser. Specifically, we investigate how the spe-

cialist neural network and the bidirectional feedback loop influence the final performance.

4.2.1 Multimodal Representation Alignment

We compare the accuracy and completeness of geometric information extracted by the MLLM equipped with PGDPNet against few-shot MLLM extraction. Evaluations are conducted on Qwen3-VL-32B, Qwen3-VL-Plus, GPT-4o and BiNSGPS on a randomly chosen 100 scale subset of Geometry3K dataset. The results are reported in Table 2.

As shown in Table 2, general-purpose MLLMs frequently struggle to reach 60% alignment accuracy. This is largely due to "semantic hallucinations," where the models overlook fine-grained geometric details or fail to capture the complete set of relations in diagrams. In contrast, BiNSGPS achieves an alignment accuracy of 80.0%. This significant gain is attributed to the using of PGDPNet. By giving the extraction of basic geometric elements and spatial relationships to a dedicated network, we transform visually dense diagrams into high-fidelity symbolic primitives. This decoupling allows the MLLM to focus instead on identifying high-level geometric properties. By providing the MLLM with an "anchored" foundation of basic elements, we effectively mitigate the "perceptual drift" typical of pure-neural approaches, ensuring that the initial representation set \mathcal{L} is both comprehensive and mathematically grounded.

Table 3: Ablation study of MLLM Adviser.

Method	Geometry3K	PGPS9K
No MLLM Adviser	73.3%	72.1%
rectify-only	80.4%	75.6%
hypothesis-only	77.6%	79.2%
BiNSGPS	90.5%	90.1%

4.2.2 MLLM Adviser and Feedback

To isolate the impact of the bidirectional feedback loop, we compare the full BiNSGPS framework against an ablated version lacking the MLLM Adviser. In this "No Adviser" configuration, the system functions as an unidirectional pipeline. We also provide the data about only keep one function of MLLM Adviser as "rectify-only" and "hypothesis-only". The results are summarized in Table 3.

As shown in the Table 3, the inclusion of the MLLM Adviser yields a transformative improvement in answer accuracy, with gains of 17.2% on Geometry3K and 18.0% on PGPS9K in Completion mode. This performance surge is primarily

driven by two synergistic functions: Iterative Error Recovery, where the MLLM uses diagnostic feedback to rectify initial parsing hallucinations; Knowledge Augmentation, which allows the system to bypass theorem-set limitations by proposing auxiliary hypotheses; By transforming the Symbolic Solver from a passive executor into an active diagnostic partner, BiNSGPS overcomes the brittleness inherent in traditional neuro-symbolic systems, establishing a new ceiling for geometry problem-solving performance.

4.3 Iteration Rounds

To evaluate the efficiency of the Bidirectional Neuro-Symbolic Interaction (BiNS), we analyze the number of rounds required by the MLLM Adviser to reach a valid solution. In our framework, we implement a safety threshold with a maximum iteration limit of $T = 3$. The empirical distribution of success rounds using Qwen3-VL-Plus as MLLM Adviser, as illustrated in Fig. 3(b), demonstrates the rapid convergence of the BiNS loop. Among the cases requiring intervention beyond the initial formalization, the system successfully resolves 171 problems in a single iteration, 77 cases in two iterations, and 35 cases in three iterations(Fallback).

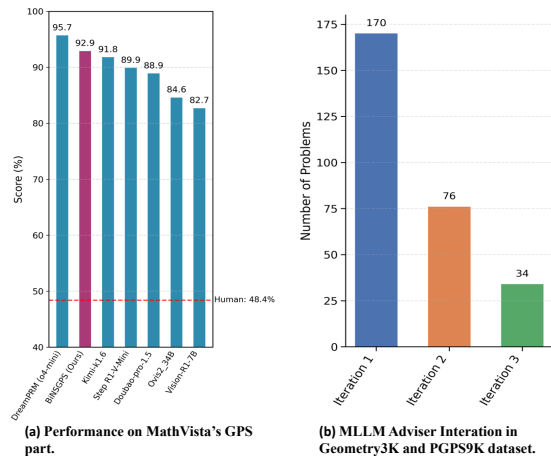


Figure 3: Performance in MathVista (a) and Adviser Iteration in Geometry3K and PGPS9K dataset (b).

The high early success rate reflects the precision of the Symbolic Solver's diagnostic feedback. By identifying exact symbolic conflicts, it enables targeted corrections instead of stochastic search. Few cases require a third iteration, confirming efficient mastery of complex reasoning without excessive computation. This validates BiNSGPS as a practical geometry-solving paradigm, balancing multimodal intuition with rapid symbolic verification.

5 Conclusion

This paper introduces BiNSGPS, a framework that reformulates the neuro-symbolic architecture through Bidirectional Neuro-Symbolic Interaction (BiNS). By establishing a closed-loop feedback mechanism between an MLLM Adviser and a Symbolic Solver, we enable the system to iteratively rectify formal representations and propose auxiliary hypotheses, effectively synergizing the adaptive intuition of neural models with the mathematical rigor of symbolic reasoning.

Limitations

While BiNSGPS achieves state-of-the-art performance on Geometry3K and PGPS9K, we identify the automated generation of auxiliary constructions as a key frontier for the next iteration of neuro-symbolic reasoning. Currently, the Geometry3K and PGPS9K datasets impose minimal requirements for auxiliary points and lines. Consequently, we deliberately refrain from prompting the MLLM to generate such elements to mitigate potential hallucinations. In addition, although we use prompts to control the output of MLLMs, in certain cases, MLLMs may lose control and repeatedly doubt their previous reasoning steps, leading to excessively long outputs. Further research is needed to enhance the controllability of MLLMs.

References

- Shuai Bai, Yuxuan Cai, Ruizhe Chen, Keqin Chen, Xionghui Chen, Zesen Cheng, Lianghao Deng, Wei Ding, Chang Gao, Chunjiang Ge, and 1 others. 2025. Qwen3-vl technical report. *arXiv preprint arXiv:2511.21631*.
- Shihao Cai, Keqin Bao, Hangyu Guo, Jizhi Zhang, Jun Song, and Bo Zheng. 2024. *Geogpt4v: Towards geometric multi-modal large language models with geometric image generation*. *Preprint*, arXiv:2406.11503.
- Jiaqi Chen, Tong Li, Jinghui Qin, Pan Lu, Liang Lin, Chongyu Chen, and Xiaodan Liang. 2022. *Unigeo: Unifying geometry logical reasoning via reformulating mathematical expression*. *Preprint*, arXiv:2212.02746.
- Jiaqi Chen, Jianheng Tang, Jinghui Qin, Xiaodan Liang, Lingbo Liu, Eric Xing, and Liang Lin. 2021. *Geoqa: A geometric question answering benchmark towards multimodal numerical reasoning*. In *Findings of the Association for Computational Linguistics: ACL-IJCNLP 2021*, pages 513–523.
- Yi Chen, Jian Xu, Xu-Yao Zhang, Wen-Zhuo Liu, Yang-Yang Liu, and Cheng-Lin Liu. 2025. Recoverable compression: A multimodal vision token recovery mechanism guided by text information. In *Proceedings of the AAAI Conference on Artificial Intelligence*, volume 39, pages 2293–2301.
- Yuri Chervonyi, Trieu H. Trinh, Miroslav Olšák, Xiaomeng Yang, Hoang Nguyen, Marcelo Menegali, Junehyuk Jung, Junsu Kim, Vikas Verma, Quoc V. Le, and Thang Luong. 2025. *Gold-medalist performance in solving olympiad geometry with alphageometry2*. *Preprint*, arXiv:2502.03544.
- Chengqi Duan, Kaiyue Sun, Rongyao Fang, Manyuan Zhang, Yan Feng, Ying Luo, Yufang Liu, Ke Wang, Peng Pei, Xunliang Cai, Hongsheng Li, Yi Ma, and Xihui Liu. 2025. *Codeplot-cot: Mathematical visual reasoning by thinking with code-driven images*. *Preprint*, arXiv:2510.11718.
- Daocheng Fu, Jianlong Chen, Renqiu Xia, Zijun Chen, Qi Liu, Yuan Feng, Hongbin Zhou, Renrui Zhang, Shiyang Feng, Peng Gao, and 1 others. 2025a. Trustgeogen: Formal-verified data engine for trustworthy multi-modal geometric problem solving. *arXiv preprint arXiv:2504.15780*.
- Yumeng Fu, Jiayin Zhu, Lingling Zhang, Bo Zhao, Shaoxuan Ma, Yushun Zhang, Yanrui Wu, and Wenjun Wu. 2025b. *Geolaux: A benchmark for evaluating mllms' geometry performance on long-step problems requiring auxiliary lines*. *Preprint*, arXiv:2508.06226.
- Wenbin Gan and Xinguo Yu. 2018. *Automatic understanding and formalization of natural language geometry problems using syntax-semantics models*. *International Journal of Innovative Computing, Information and Control*, 14:83–98.
- Jiahui Gao, Renjie Pi, Jipeng Zhang, Jiacheng Ye, Wan-jun Zhong, Yufei Wang, Lanqing Hong, Jianhua Han, Hang Xu, Zhenguo Li, and 1 others. 2023. *G-llava: Solving geometric problem with multi-modal large language model*. *arXiv preprint arXiv:2312.11370*.
- Zhangwei Gao, Zhe Chen, Erfei Cui, Yiming Ren, Weiyun Wang, Jinguo Zhu, Hao Tian, Shenglong Ye, Junjun He, Xizhou Zhu, Lewei Lu, Tong Lu, Yu Qiao, Jifeng Dai, and Wenhai Wang. 2024. *Mini-internvl: A flexible-transfer pocket multimodal model with 5% parameters and 90% performance*. *Preprint*, arXiv:2410.16261.
- Zhibin Gou, Zhihong Shao, Yeyun Gong, Yelong Shen, Yujia Yang, Minlie Huang, Nan Duan, and Weizhu Chen. 2024. *Tora: A tool-integrated reasoning agent for mathematical problem solving*. In *International Conference on Learning Representations*, volume 2024, pages 48362–48395.
- Yushi Hu, Weijia Shi, Xingyu Fu, Dan Roth, Mari Ostendorf, Luke Zettlemoyer, Noah A Smith, and Ranjay Krishna. 2024. *Visual sketchpad: Sketching as a*

- visual chain of thought for multimodal language models. In *Advances in Neural Information Processing Systems*, volume 37, pages 139348–139379. Curran Associates, Inc.
- Wenxuan Huang, Bohan Jia, Zijie Zhai, Shaosheng Cao, Zheyu Ye, Fei Zhao, Zhe Xu, Yao Hu, and Shaohui Lin. 2026. Vision-r1: Incentivizing reasoning capability in multimodal large language models. *Preprint*, arXiv:2503.06749.
- Zenan Li, Yifan Wu, Zhaoyu Li, Xinming Wei, Fan Yang, Xian Zhang, and Xiaoxing Ma. 2024a. Autoformalize mathematical statements by symbolic equivalence and semantic consistency. In *Advances in Neural Information Processing Systems*, volume 37, pages 53598–53625. Curran Associates, Inc.
- Zhong-Zhi Li, Ming-Liang Zhang, Fei Yin, and Cheng-Lin Liu. 2024b. LANS: A layout-aware neural solver for plane geometry problem. In *Findings of the Association for Computational Linguistics: ACL 2024*, pages 2596–2608, Bangkok, Thailand. Association for Computational Linguistics.
- Pan Lu, Hritik Bansal, Tony Xia, Jiacheng Liu, Chunyuan Li, Hannaneh Hajishirzi, Hao Cheng, Kai-Wei Chang, Michel Galley, and Jianfeng Gao. 2024. Mathvista: Evaluating mathematical reasoning of foundation models in visual contexts. In *International Conference on Learning Representations*, volume 2024, pages 23439–23554.
- Pan Lu, Ran Gong, Shibiao Jiang, Liang Qiu, Siyuan Huang, Xiaodan Liang, and Song-Chun Zhu. 2021. Inter-gps: Interpretable geometry problem solving with formal language and symbolic reasoning. In *Proceedings of the 59th Annual Meeting of the Association for Computational Linguistics and the 11th International Joint Conference on Natural Language Processing (Volume 1: Long Papers)*, pages 6774–6786.
- Maizhen Ning, Zihao Zhou, Qiufeng Wang, Xiaowei Huang, and Kaizhu Huang. 2025. Gns: Solving plane geometry problems by neural-symbolic reasoning with multi-modal llms. In *Proceedings of the AAAI Conference on Artificial Intelligence*, volume 39, pages 24957–24965.
- OpenAI. 2024. Gpt-4o system card. *Preprint*, arXiv:2410.21276.
- Liangming Pan, Alon Albalak, Xinyi Wang, and William Wang. 2023. Logic-LM: Empowering large language models with symbolic solvers for faithful logical reasoning. In *Findings of the Association for Computational Linguistics: EMNLP 2023*, pages 3806–3824, Singapore. Association for Computational Linguistics.
- Shuai Peng, Di Fu, Yijun Liang, Liangcai Gao, and Zhi Tang. 2023. GeoDRL: A self-learning framework for geometry problem solving using reinforcement learning in deductive reasoning. In *Findings of the Association for Computational Linguistics: ACL 2023*, pages 13468–13480, Toronto, Canada. Association for Computational Linguistics.
- Bowen Ping, Minnan Luo, Zhuohang Dang, Chenxi Wang, and Chengyou Jia. 2025. Autogps: Automated geometry problem solving via multimodal formalization and deductive reasoning. *Preprint*, arXiv:2505.23381.
- Qwen, :, An Yang, Baosong Yang, Beichen Zhang, Binyuan Hui, Bo Zheng, Bowen Yu, Chengyuan Li, Dayiheng Liu, Fei Huang, Haoran Wei, Huan Lin, Jian Yang, Jianhong Tu, Jianwei Zhang, Jianxin Yang, Jiayi Yang, Jingren Zhou, and 25 others. 2025. Qwen2.5 technical report. *Preprint*, arXiv:2412.15115.
- Zhihong Shao, Yuxiang Luo, Chengda Lu, Z. Z. Ren, Jiewen Hu, Tian Ye, Zhibin Gou, Shirong Ma, and Xiaokang Zhang. 2025. Deepseekmath-v2: Towards self-verifiable mathematical reasoning. *Preprint*, arXiv:2511.22570.
- Zhihong Shao, Peiyi Wang, Qihao Zhu, Runxin Xu, Junxiao Song, Xiao Bi, Haowei Zhang, Mingchuan Zhang, Y. K. Li, Y. Wu, and Daya Guo. 2024. Deepseekmath: Pushing the limits of mathematical reasoning in open language models. *Preprint*, arXiv:2402.03300.
- Wenhao Shi, Zhiqiang Hu, Yi Bin, Junhua Liu, Yang Yang, See Kiong Ng, Lidong Bing, and Roy Ka-Wei Lee. 2024. Math-llava: Bootstrapping mathematical reasoning for multimodal large language models. In *Findings of the Association for Computational Linguistics: EMNLP 2024*, pages 4663–4680.
- Dídac Surís, Sachit Menon, and Carl Vondrick. 2023. Vipergpt: Visual inference via python execution for reasoning. In *Proceedings of the IEEE/CVF International Conference on Computer Vision (ICCV)*, pages 11888–11898.
- Trieu Trinh, Yuhuai Wu, Quoc Le, He He, and Thang Luong. 2024. Solving olympiad geometry without human demonstrations. *Nature*.
- Ke Wang, Junting Pan, Weikang Shi, Zimu Lu, Houxing Ren, Aojun Zhou, Mingjie Zhan, and Hongsheng Li. 2024. Measuring multimodal mathematical reasoning with math-vision dataset. In *Advances in Neural Information Processing Systems*, volume 37, pages 95095–95169. Curran Associates, Inc.
- Peijie Wang, Zhong-Zhi Li, Fei Yin, Dekang Ran, and Cheng-Lin Liu. 2025a. Mv-math: Evaluating multimodal math reasoning in multi-visual contexts. In *Proceedings of the Computer Vision and Pattern Recognition Conference*, pages 19541–19551.
- Peijie Wang, Chao Yang, Zhong-Zhi Li, Fei Yin, Dekang Ran, Mi Tian, Zhilong Ji, Jinfeng Bai, and Cheng-Lin Liu. 2025b. Solidgeo: Measuring multimodal spatial math reasoning in solid geometry. *arXiv preprint arXiv:2505.21177*.

- Peijie Wang, Ming-Liang Zhang, Jun Cao, Chao Deng, Dekang Ran, Hongda Sun, Pi Bu, Xuan Zhang, Yingyao Wang, Jun Song, and 1 others. 2026. Geoparsing: Diagram parsing for plane and solid geometry with a unified formal language. *arXiv preprint arXiv:2604.11600*.
- Wenjun Wu, Lingling Zhang, Jun Liu, Xi Tang, Yaxian Wang, Shaowei Wang, and Qianying Wang. 2024. E-gps: Explainable geometry problem solving via top-down solver and bottom-up generator. In *2024 IEEE/CVF Conference on Computer Vision and Pattern Recognition (CVPR)*, pages 13828–13837.
- Yuhuai Wu, Albert Qiaochu Jiang, Wenda Li, Markus Rabe, Charles Staats, Mateja Jamnik, and Christian Szegedy. 2022. Autoformalization with large language models. In *Advances in Neural Information Processing Systems*, volume 35, pages 32353–32368. Curran Associates, Inc.
- Fangzhi Xu, Qiushi Sun, Kanzhi Cheng, Jun Liu, Yu Qiao, and Zhiyong Wu. 2024a. Interactive evolution: A neural-symbolic self-training framework for large language models. *Preprint*, arXiv:2406.11736.
- Fangzhi Xu, Zhiyong Wu, Qiushi Sun, Siyu Ren, Fei Yuan, Shuai Yuan, Qika Lin, Yu Qiao, and Jun Liu. 2024b. Symbol-LLM: Towards foundational symbol-centric interface for large language models. In *Proceedings of the 62nd Annual Meeting of the Association for Computational Linguistics (Volume 1: Long Papers)*, pages 13091–13116, Bangkok, Thailand. Association for Computational Linguistics.
- Xiao-Wen Yang, Jie-Jing Shao, Lan-Zhe Guo, Bo-Wen Zhang, Zhi Zhou, Lin-Han Jia, Wang-Zhou Dai, and Yu-Feng Li. 2025. Neuro-symbolic artificial intelligence: towards improving the reasoning abilities of large language models. In *Proceedings of the Thirty-Fourth International Joint Conference on Artificial Intelligence*, pages 10770–10778.
- yi chen, Yu Zhang, Jian Xu, Hua Yue, Xinming Wang, Zequan Lyu, Xu-Yao Zhang, Wei Wei, and Cheng-Lin Liu. 2026. An open-ended benchmark and formal framework for adjuvant research with MLLM. In *The Fourteenth International Conference on Learning Representations*.
- Chi Zhang, Jiajun Song, Siyu Li, Yitao Liang, Yuxi Ma, Wei Wang, Yixin Zhu, and Song-Chun Zhu. 2024a. Proposing and solving olympiad geometry with guided tree search. *Preprint*, arXiv:2412.10673.
- Jiaxin Zhang, Zhong-Zhi Li, Ming-Liang Zhang, Fei Yin, Cheng-Lin Liu, and Yashar Moshfeghi. 2024b. Geoeval: benchmark for evaluating llms and multimodal models on geometry problem-solving. In *Findings of the Association for Computational Linguistics: ACL 2024*, pages 1258–1276.
- Ming-Liang Zhang, Zhong-Zhi Li, Fei Yin, Liang Lin, and Cheng-Lin Liu. 2024c. Fuse, reason and verify: Geometry problem solving with parsed clauses from diagram. *Preprint*, arXiv:2407.07327.
- Ming-Liang Zhang, Fei Yin, Yi-Han Hao, and Cheng-Lin Liu. 2022. Plane geometry diagram parsing. In *Proceedings of the Thirty-First International Joint Conference on Artificial Intelligence, IJCAI-22*, pages 1636–1643. International Joint Conferences on Artificial Intelligence Organization. Main Track.
- Ming-Liang Zhang, Fei yin, and Cheng-Lin Liu. 2023. A multi-modal neural geometric solver with textual clauses parsed from diagram. In *Proceedings of the Thirty-Second International Joint Conference on Artificial Intelligence, IJCAI-23*, pages 3374–3382. International Joint Conferences on Artificial Intelligence Organization. Main Track.
- Xiaokai Zhang, Yang Li, Na Zhu, Cheng Qin, Zhenbing Zeng, and Tuo Leng. 2025. Fgeo-hypergnet: Geometric problem solving integrating formalgeo symbolic system and hypergraph neural network. In *Proceedings of the Thirty-Fourth International Joint Conference on Artificial Intelligence, IJCAI-25*, pages 4733–4741. International Joint Conferences on Artificial Intelligence Organization. Main Track.
- Xiaokai Zhang, Na Zhu, Yiming He, Jia Zou, Qike Huang, Xiaoxiao Jin, Yanjun Guo, Chenyang Mao, Yang Li, Zhe Zhu, Dengfeng Yue, Fangzhen Zhu, Yifan Wang, Yiwen Huang, Runan Wang, Cheng Qin, Zhenbing Zeng, Shaorong Xie, Xiangfeng Luo, and Tuo Leng. 2024d. Formalgeo: An extensible formalized framework for olympiad geometric problem solving. *Preprint*, arXiv:2310.18021.
- Junbo Zhao, Ting Zhang, Jiayu Sun, Mi Tian, and Hua Huang. 2025. Pi-gps: Enhancing geometry problem solving by unleashing the power of diagrammatic information. *Preprint*, arXiv:2503.05543.
- Jinguo Zhu, Weiyun Wang, Zhe Chen, Zhaoyang Liu, Shenglong Ye, Lixin Gu, Hao Tian, Yuchen Duan, Weijie Su, Jie Shao, Zhangwei Gao, Erfei Cui, Xuehui Wang, Yue Cao, Yangzhou Liu, Xingguang Wei, Hongjie Zhang, Haomin Wang, Weiye Xu, and 32 others. 2025. Internvl3: Exploring advanced training and test-time recipes for open-source multimodal models. *Preprint*, arXiv:2504.10479.

A GPS Problem Formulation

The task of Geometry Problem Solving (GPS) is formally defined as follows. The system is provided with a dataset $\{\mathcal{D}_i, \mathcal{T}_i\}$, where \mathcal{D}_i denotes the geometric diagram, and \mathcal{T}_i denotes the corresponding textual description (e.g., "Find the measure of angle ABC"). Given both the diagram and the text, the system is required to generate the corresponding answer A_i , along with the associated solution steps $\mathcal{S} = \{s_1, s_2, \dots, s_n\}$. We evaluate the system under two primary settings. In the competition mode, problems are presented in an open-ended format where the system must directly output the final value. In the choice mode, problems are presented in a multiple-choice format, requiring the system to select the correct option from four candidates $\{\mathcal{D}_i, \mathcal{T}_i\}$.

B Experiment details

B.1 Computational Cost Analysis

To rigorously evaluate the cost introduced by our proposed framework, we conducted a detailed cost analysis on the Geometry3K and PGPS9K datasets. Our analysis reveals that the BiNS framework incurs an average computational cost of 2,634 tokens per question. This token consumption is deemed justifiable when weighed against the substantial gains in accuracy. Concurrently, the BiNSGPS framework introduces an average latency of 3.54 minutes; this temporal overhead falls well within acceptable bounds for practical deployment.

B.2 Choice Mode

In many existing geometry solvers, the presence of multiple-choice options is used to simplify the problem space via elimination or "guess-and-check" heuristics. In contrast, BiNSGPS maintains a "completion-first" philosophy, where the choices serve exclusively as a Consistency Check within the bidirectional loop.

The transition from standard deduction to Choice-based rectification follows a strict logical sequence: The Symbolic Solver first attempts to derive a solution S_{sym} using only the formal representations \mathcal{L} and theorems \mathcal{R} , without access to the candidate options $\{A, B, C, D\}$. If S_{sym} does not align with any of the candidate choices, the system identifies a symbolic-perceptual mismatch. This discrepancy acts as the trigger for the MLLM Adviser. The Adviser is then provided with the candidate choices as auxiliary constraints.

A primary advantage of this approach is its ability to prevent the system from "guessing" based on visual intuition or heuristic shortcuts. While pure MLLMs often select an option based on plausible, BiNSGPS instead treats the choice set as a high-level diagnostic signal to re-examine the answer. This ensures that the final selection is not merely a statistical probability but is always supported by a valid symbolic proof chain derived through the Solver.

B.3 Fallback rate and Accuracy

To clarify the influence of fallback mode, we analyse the trigger frequency and accuracy of fallback mode. Across the two datasets, only 105 questions triggered BiNSGPS's fallback mode, accounting for just 6.56% of the datasets. And the accuracy in fallback mode is 33.3%. This accuracy is largely due to the questions that can't be solved in normal mode are the hardest part of the datasets and MLLM Adviser can hardly handle them, the accuracy of Qwen3-VL-Plus in these question is 29.5%, also largely lower than the average level. But as stated in the paper, the fallback mode mainly serves as a robustness safeguard, ensuring that BiNSGPS can still return an answer instead of collapsing without output.

B.4 PGDPNet

The reliability of a neuro-symbolic system depends heavily on the accuracy of its initial perception layer. In BiNSGPS, we utilize PGDPNet as our specialist neural network for diagram parsing to ensure the initial formal representation set \mathcal{L} is mathematically grounded. To justify its role as a robust "anchor" for our experiments, we provide its performance metrics on geometric primitive detection and spatial relationship extraction below.

As summarized in Table 4, PGDPNet achieves near-perfect scores across all primary geometric primitives.

Table 4: PGDPNet Precision, Recall, and F1 Score for Primitive Detection

Primitive	Precision (%)	Recall (%)	F1 Score (%)
Point	99.65	99.71	99.68
Line	99.30	99.51	99.40
Circle	99.85	99.96	99.90

Beyond identifying isolated primitives, PGDPNet is tasked with extracting topological relations such as tangency, collinearity, and intersections.

For these complex positional relationships, the model achieves a Precision of 99.13%, a Recall of 98.60%, and an F1 Score of 98.86%.

These metrics demonstrate that PGDPNet provides an exceptionally sound foundation for the BiNSGPS pipeline. By maintaining 99%+ accuracy in primitive detection, the network minimizes the "noise" typically introduced by general-purpose MLLMs.

C Symbolic Solver

C.1 Theorems Apply Strategy

To maximize problem-solving performance, the Symbolic Solver employs a complexity-ascending heuristic that orchestrates theorem application strictly according to the cardinality of their required conditions. This strategic ordering is paramount for system efficacy; given that deeper conclusions frequently depend on the derivation of intermediate results, an ill-sequenced application order can precipitate premature termination, thereby preventing the system from converging upon the final solution within the stipulated iteration limit.

C.2 The Minimal Solution Graph

Minimal solution graph is the reference for proof generation. Thanks to the hypergraph-based solving process, Solver can track the trace of prove. The Symbolic Solver performs a recursive backtrace from the destination node to its fundamental root nodes within the hypergraph. In hypergraph expansion, every node except the initial ones records the theorems and predecessor nodes utilized during reasoning. By backtracking from the final node, the Symbolic Solver can trace all necessary paths from the root to the target node, thereby enabling the identification of the Minimal Solution Graph. This extraction identifies the minimal solution graph, filtering out redundant derivations to ensure a concise and step-wise logical path.

C.3 Rule-based Filter

To ensure the output remains within the permitted logic space of the symbolic engine, BiNSGPS utilizes a Rule-Based Filter that acts as a deterministic security layer. This filter provides a lightweight yet robust mechanism to validate representations before send to solver.

The filter permits Algebraic and Trigonometric Rules. It validates Basic Elements as defined in the primary representation space and accepts Fundamental Operators such as Equals and Find. Quan-

titative Attributes are strictly limited to AreaOf, RadiusOf, MeasureOf, and LengthOf. Finally, Geometric Relations are restricted to a high-fidelity subset: Parallel, Perpendicular, IsSimilarity, IsCongruent, Tangent, IsMidpointOf, and IsMidsegmentOf.

In the Multimodal Representations Alignment stage, if a non-compliant or hallucinated assertion is detected, the checker provides immediate feedback, prompting the MLLM to regenerate the representation. This multi-layered verification transforms each problem $(\mathcal{D}_i, \mathcal{T}_i)$ into a logically consistent initial representation set \mathcal{L}_i , ready for Symbolic Solver's rigorous deduction.

We also implement a rule-based filter that acts as a syntactic gateway between the MLLM Adviser and the Symbolic Solver. This filter automatically screens and excludes any generated assertions that fall outside the solver's permissible assertion space, effectively neutralizing the risk of format-induced failures. It also verifies that every referenced point and circle corresponds to an entity already identified in the initial formalization, preventing the MLLM from hallucinating non-existent vertices or primitives.

By operating as a rigid pattern-matching gateway, the filter ensures that the BiNSGPS remains mathematically sound, protecting the Symbolic Solver from the inherent stochasticity of neural model outputs.

C.4 Formal Representation Definitions

To ensure a rigorous interface between the MLLM and the symbolic engine, BiNSGPS utilizes a structured representation space. Following the principles of AutoGPS, we categorize these logic forms into two primary groups: basic structural foundations and high-level geometric constraints.

The first Table 5 comprises Basic Elements and Algebraic Rules, which define the existence of geometric primitives (Points, Lines, Circles, Polygons) and the fundamental arithmetic operations used to model their numerical relationships. The second Table 6 consists of Relations and Quantitative Attributes, which describe how these primitives interact (e.g., parallelism, tangency, or collinearity) and define their measurable properties such as length, angle measure, and area.

By mapping multimodal inputs to this standardized space, the framework ensures that every step taken by the Symbolic Solver is grounded in a formal axiomatic system. This structured approach allows the MLLM Adviser to perform rectifications

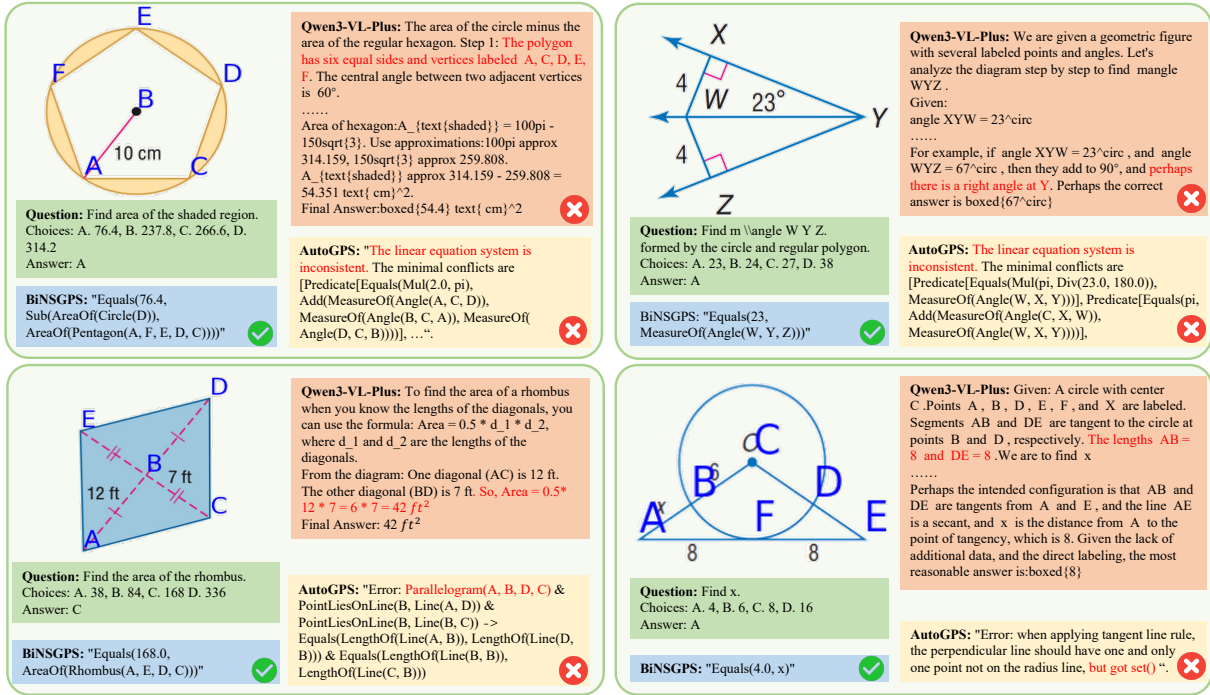


Figure 4: Failure cases of current methods. Qwen3-VL-Plus exhibits hallucination induced errors during reasoning (up-left: recognize pentagon as hexagon), producing an incorrect conclusion. The neural-symbolic method (AutoGPS) will immediately fail when the logic forms have conflict. While BiNSGPS show more robustness with MLLM’s feedback. Red annotations indicate correct/erroneous reasoning or answers.

by targeting specific predicates in the logic set.

D Feedback mode

We acknowledge that AutoGPS also incorporates feedback, but its mechanism is fundamentally performs one-time, pre-reasoning validation of formalized representations: once the initial representation passes the self-consistency check, the loop terminates permanently. Consequently, even if the formalization is initially deemed consistent, hidden contradictions may still emerge during deduction, and AutoGPS has no mechanism to recover. In contrast, BiNSGPS establishes a runtime cognitive collaboration: when the symbolic solver encounters conflicts or deadlocks during reasoning, the MLLM Adviser intervenes to perform diagnostic correction guided by derived contradictions, or to propose auxiliary theorems that serve as new deductive steps to resolve the impasse. We elevate the MLLM from a one-time validator to a collaborative partner throughout the entire proof search, and this architectural shift is what drives the substantial performance gain.

E Case Study

To provide a more comprehensive illustration of the efficacy and limitations of our proposed method,

we present a series of case studies herein.

E.1 Illustrative Case

We present illustrative case studies in Fig. 4 to demonstrate the BiNSGPS’s performance on diverse geometry problems and show its advantages over other methods.

E.2 Success Case

Here we present detailed example of BiNSGPS’s success case to illustrate our framework’s effect. The success of BiNSGPS is defined by its ability to resolve representational conflicts and leverage symbolic feedback. The system successfully recovers from initial formalization errors and overcomes limitation by proposing auxiliary hypotheses as shown in Fig. 5 and Fig. 6

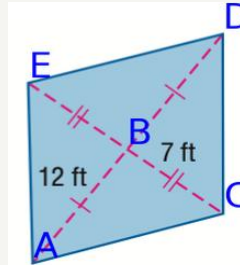
E.3 Fail Cases

Here we present the failure cases of BiNSGPS as shown in Fig. 7. For the correct results but wrong steps, MLLM Adviser fails to assign value to corresponding element but drives the right answer in coincidence. For the fail case, the diagram usually contains too many element that MLLM Adviser can hardly detect them, and leads to failure.

Result of BiNSGPS on Geometry3K sample

Question: Find the area of the rhombus.

- A. 38
- B. 84
- C. 168
- D. 336



Ground Truth: C

Initial Logic Forms:

```
"PointLiesOnLine(B, Line(D, A))",
"PointLiesOnLine(B, Line(E, C))",
"Equals(LengthOf(Line(B, C)), LengthOf(Line(E, B)))",
"Equals(LengthOf(Line(C, B)), 7)",
"Equals(LengthOf(Line(D, B)), LengthOf(Line(B, A)))",
"Equals(LengthOf(Line(E, A)), 12)",
"Find(AreaOf(Rhombus(A, B, C, D)))"
```

Error: Premise nodes are not in the graph - [Predicate[PointLiesOnLine(B, Line(B, C))]] when connecting with theorem Parallelogram Diagonals Bisect ... ❌

MLLM Adviser:

The error was in the premise PointLiesOnLine(B, Line(B, C)), which is invalid because a point cannot lie on a line segment from itself to itself. This was incorrect.

...

Re-examining the image: B is the intersection point of diagonals.

So B is not a vertex — this contradicts the name "Rhombus(A, B, C, D)".

Ah! Critical issue: B is the center, not a vertex.

...

Note: Original had Rhombus(A, B, C, D) — now corrected to Rhombus(A, E, D, C)

Answer: "Equals(168.0, AreaOf(Rhombus(A, E, D, C)))" ✓

Step 1: Identify the diagonals

The rhombus has diagonals AD and EC , intersecting at point B .

Since diagonals of a rhombus bisect each other:

$$AB = BD = 12 \text{ ft} \Rightarrow AD = 24 \text{ ft}, EB = BC = 7 \text{ ft} \Rightarrow EC = 14 \text{ ft}$$

Step 2: Use the rhombus area formula

For any rhombus, the area is half the product of its diagonals:

$$\text{Area} = \frac{1}{2} \cdot d_1 \cdot d_2$$

Step 3: Substitute known lengths

$$\text{Area} = \frac{1}{2} \cdot 24 \cdot 14 = \frac{336}{2} = 168 \text{ ft}^2$$

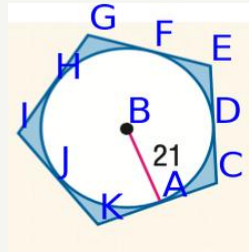
Figure 5: Success case of BiNSGPS's Rectify Inconsistent Representations.

Result of BiNSGPS on Geometry3K sample

Question: Find the area of the shaded region.

- A. 216.6
- B. 282.9
- C. 464.8
- D. 819.6

Ground Truth: A



Initial Logic Forms:

```
"PointLiesOnCircle(A, Circle(B))", "PointLiesOnCircle(D, Circle(B))",
...
"Equals(LengthOf(Line(B, A)), 21)", "Regular(Pentagon(A, D, F, H, J))",
"Find(Sub(AreaOf(Circle(B)), AreaOf(Pentagon(A, D, F, H, J)))"
```

Error: The symbolic System cannot solve the question, please give the hypothesis.

MLLM Adviser:

We are given a diagram involving a regular pentagon inscribed in a circle, with the center of the circle labeled as B, and a radius BA=21.

The only resolution is that the **circle is inscribed**, and A is not a vertex, but the logic form is wrong. Given the diagram shows the circle inside the pentagon, and A is on the circle and on a side, A is a **point of tangency**, not a vertex. Shaded area = Area(pentagon) - Area(circle).

Final Logic Forms:

```
"Equals(RadiusOf(Circle(B)), 21)",
"Equals(AreaOf(Pentagon(C, E, G, I, K)), Mul(5, Pow(21, 2), Tan(Div(Pi, 5))))",
"Find(Sub(AreaOf(Pentagon(C, E, G, I, K)), AreaOf(Circle(B)))"
```

Answer: Equals(216.6, Sub(AreaOf(Pentagon(C, E, G, I, K)), AreaOf(Circle(B)))) ✓

Step 1: Area of the Circle

The circle has radius $r = 21$, so: $A_{circle} = \pi r^2 = \pi \cdot 21^2 = 441\pi$

Step 2: Area of the Regular Pentagon (given inradius r)

For any regular n -gon with **inradius** (apothem) r , the area is: $A = \frac{1}{2} \cdot P \cdot r$

where P is the perimeter....

Perimeter: $P = 10r \tan\left(\frac{\pi}{5}\right)$

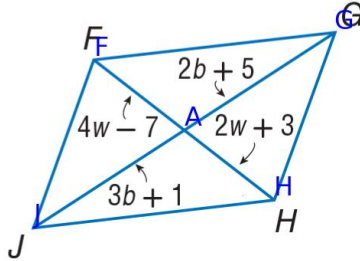
Step 3: Shaded Area

$$A_{shaded} = A_{pentagon} - A_{circle} \approx 216.6$$

Figure 6: Success case of BiNSGPS's Propose Auxiliary Hypotheses.

Correct result but wrong steps

Question: Find w in the given parallelogram.
 Choices: A. 3.0, B. 4.0, C. 5.0, D. 13.0
 Answer: C



```
"logic_forms": [
  "Equals(LengthOf(Line(F, A)), 4w-7)",
  "Equals(LengthOf(Line(F, G)), 2b+5)",
  "Equals(LengthOf(Line(G, A)), 2w+3)",
  "Equals(LengthOf(Line(J, H)), 3b+1)"
]
```

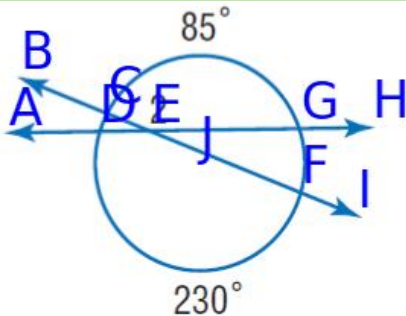
MLLM Adviser: "Based on the image and the provided symbolic logic forms, we analyze the parallelogram JFGH with diagonals intersecting at point A. We observe: The segments from the intersection point A to the vertices are labeled: $FA=4w-7$, $GA=2w+3$, $HA=3b+1$, $JA=2b+5$. So, by diagonal bisection, we get
 (1) $4w-7 = 3b+1$,
 (2) $2w+3 = 2b+5$,
 These two equations can be solved simultaneously to find w ."

```
"refined_logic_forms": [
  "Parallelogram(J, F, G, H)",
  "Equals(LengthOf(Line(F, A)), 4w - 7)",
  "Equals(LengthOf(Line(H, A)), 3b + 1)",
  "Equals(LengthOf(Line(G, A)), 2w + 3)",
  "Equals(LengthOf(Line(J, A)), 2b + 5)",
  ...
]
```

BiNSGPS: "Equals(5.0, w)"

Fail Case

Question: Find the measure of angle 2.
 Choices: A. 85, B. 157.5, C. 230, D. 315
 Answer: B



```
"logic_forms": [
  "Equals(MeasureOf(Angle(G, E, C)), MeasureOf(angle 2))",
  "Equals(MeasureOf(Arc(F, G)), 230)",
  "Equals(MeasureOf(Arc(C, G)), 85)",
  "Tangent(Line(A, E), Circle(J))",
  "Tangent(Line(B, I), Circle(J))"
]
```

Error: These symbolic language representation cause error: The tangent line Line(B, I) intersects with the circle Circle(J) at more than one point

MLLM Adviser: "The error in the symbolic representation arises from the statement:
 $Tangent(Line(B, I), Circle(J, radius_0_0))$
 This is incorrect because line BI intersects the circle at two points (F and G), as seen in the image. So remove invalid tangent."

```
"refined_logic_forms": [
  "Equals(MeasureOf(Angle(G, E, C)), MeasureOf(angle 2))",
  "Equals(MeasureOf(Arc(F, G)), 230)",
  "Equals(MeasureOf(Arc(C, G)), 85)",
  "Tangent(Line(A, E), Circle(J))",
]
```

Error: These symbolic language representation cause error: The tangent line Line(D, G) intersects with the circle Circle(J) at more than one point.

MLLM Adviser: "The earlier correction missed that Line(D, G) is the one incorrectly labeled as tangent. Let's re-express based on the image
 Circle centered at J.
 Horizontal line passes through D-E-J-G-H (a secant line intersecting circle at D and G).
 Line AE touches circle at E only → likely tangent at E.
 Line BI passes through F and G → secant.
 ...

```
Final Corrected Symbolic Forms:[
  "Equals(MeasureOf(Angle(G, E, C)), MeasureOf(angle 2))",
  "Equals(MeasureOf(Arc(C, G)), 85)",
  "Equals(MeasureOf(Arc(F, G)), 230)",
  "Find(MeasureOf(Angle(G, E, C)))",
  "Tangent(Line(A, E), Circle(J))",
  "Chord(Segment(D, G), Circle(J))"
]
```

Error: These symbolic language representation cause error: The tangent line Line(D, G) intersects with the circle Circle(J) at more than one point. Entering fall back mode. Please give the answer of this question with analyze-answer-proof format.

MLLM Adviser: "We are given:
 A circle with center J, Two arcs: $CG = 85$, $FG = 230$.
 Lines: AE is tangent to the circle at point E. DG is a chord intersecting circle at D and G.
 ...
 Answer: $Equals(42.5, MeasureOf(angle 2))$.
 Proof:
 Step 1: Use Tangent-Chord Angle Theorem ...
 "

BiNSGPS: "Equals(42.5, MeasureOf(angle 2))"

Figure 7: Fail cases of BiNSGPS. Including correct results but wrong steps case (up) and fail case (bottom)

Table 5: Predicate and literal definitions for the formal representations (1).

Literals	Explanation
Line(A,B)	A line segment with endpoints A and B
Angle(A)	The angle with point A as vertex
Angle(A,B,C)	Angle ABC with B as the vertex
Triangle(A,B,C)	Triangle with vertices A, B, and C
Quadrilateral(A,B,C,D)	Quadrilateral with vertices A, B, C, and D
Parallelogram(A,B,C,D)	Parallelogram with vertices A, B, C, and D
Square(A,B,C,D)	Square with vertices A, B, C, and D
Rectangle(A,B,C,D)	Rectangle with vertices A, B, C, and D
Rhombus(A,B,C,D)	Rhombus with vertices A, B, C, and D
Trapezoid(A,B,C,D)	Trapezoid with vertices A, B, C, and D
Kite(A,B,C,D)	Kite with vertices A, B, C, and D
Polygon(A,B,C,...)	Polygon with vertices A, B, C, etc.
Pentagon(A,B,C,D,E)	Pentagon with vertices A, B, C, D, and E
Hexagon(A,B,C,D,E,F)	Hexagon with vertices A, B, C, D, E, and F
Octagon(A,B,C,D,E,F,G,H)	Octagon with vertices A, B, C, D, E, F, G, and H
Circle(A)	Circle with center A
Circle(O, r)	Circle with center O and radius r
Arc(A,B)	Minor arc with A and B as endpoints on circle
Arc(A,B,C)	Arc that passes through points A, B, and C
Sector(O,A,B)	Sector of a circle with center O
SinOf(var)	Sine of var
CosOf(var)	Cosine of var
TanOf(var)	Tangent of var
CotOf(var)	Cotangent of var
HalfOf(var)	Half of var
SqrtOf(var)	Square root of var
RatioOf(var1,var2)	Ratio of var1 to var2
Add(var1,var2,...)	Addition of var1, var2 ...
Mul(var1,var2,...)	Multiplication of var1, var2, ...
Sub(var1,var2)	Subtraction of var2 from var1
Div(var1,var2)	Division of var1 by var2
Pow(var1,var2)	var1 raised to the power of var2
Equals(var1,var2)	var1 equals var2
Find(var)	Find the value of the variable

Table 6: Predicate and literal definitions for the formal representations (2).

Literals	Explanation
Equilateral(Polygon(A,B,C,D))	Polygon ABCD is equilateral
Regular(Polygon(A,B,C,D))	Polygon ABCD is regular
AreaOf(Shape(A))	Area of the Shape A
PerimeterOf(Shape(A))	Perimeter of the Shape A
RadiusOf(Circle(O))	Radius of the circle O
DiameterOf(Circle(O))	Diameter of the circle O
CircumferenceOf(Circle(O))	Circumference of the circle O
MeasureOf(Angle(A, B, C))	Measure of the angle ABC
MeasureOf(Arc(A, B))	Measure of the arc AB
LengthOf(Line(A, B))	Length of the line segment AB
PointLiesOnLine(A,Line(B,C))	Point A lies on Line BC
PointLiesOnCircle(A,Circle(O))	Point A lies on the circle O
Parallel(Line(A,B),Line(C,D))	Line AB is parallel to Line CD
Perpendicular(Line(A,B),Line(C,D))	Line AB is perpendicular to Line CD
BisectsAngle(Line(A,B),Angle(X,A,Y))	Line AB bisects angle XAY
Congruent(Triangle(A,B,C),Triangle(D,E,F))	Triangle ABC is congruent to triangle DEF
Similar(Triangle(A,B,C),Triangle(D,E,F))	Triangle ABC is similar to triangle DEF
Tangent(Line(A,B),Circle(O))	Line AB is tangent to circle O
CircumscribedTo(Shape(A),Shape(B))	Shape A is circumscribed to shape B
InscribedIn(Shape(A),Shape(B))	Shape A is inscribed in the shape B
IsMidpointOf(C,Line(A,B))	Point C is the midpoint of line AB
IsCentroidOf(O,Triangle(A,B,C))	Point O is the centroid of triangle ABC
IsIncenterOf(O,Triangle(A,B,C))	Point O is the incenter of triangle ABC
IsRadiusOf(Line(O,A),Circle(O))	Line OA is a radius of circle O
IsDiameterOf(Line(A,B),Circle(O))	Line AB is a diameter of circle O
IsMidsegmentOf(Line(A,B),Triangle(D,E,F))	Line AB is a midsegment of triangle DEF
IsPerpendicularBisectorOf(Line(A,B),Line(C,D))	Line AB is the perpendicular bisector of line CD
IsMedianOf(Line(E,F),Trapezoid(A,B,C,D))	Line EF is the median of trapezoid ABCD
IsMedianOf(Line(E,F),Triangle(A,B,C))	Line EF is a median of triangle ABC